

Searches for New Vector Like Quarks: Higgs Channels

Anupama Atre^{1*}, Mikael Chala^{2†} and José Santiago^{2‡}

¹ *Department of Physics and Astronomy,
Michigan State University,
East Lansing, MI 48824, U.S.A.*

² *CAFPE and Departamento de Física Teórica y del Cosmos,
University of Granada,
18071 Granada, Spain*

Abstract

New vector-like quarks can mix sizeably with first generation Standard Model quarks without conflicting with current experimental constraints. Searches for such new quarks have been performed in pair production and electroweak single production channels with subsequent decays into electroweak gauge bosons. To fully explore the underlying structure of the theory the channels with heavy quark decays into Higgs bosons are crucial and in this article we consider for the first time the LHC reach for such channels. The two main production mechanisms involve single production of new quarks through the fusion of a vector boson and the Higgs and single production in association with a Higgs boson. We show that both channels have promising reach at the LHC and that they complement the current direct searches involving decays into electroweak gauge bosons.

* Email: avatre@pa.msu.edu.

† Email: miki@ugr.es.

‡ Email: jsantiago@ugr.es.

I. INTRODUCTION

New vector-like quarks are a common ingredient in models of new physics. The mixing of new vector-like quarks with Standard Model (SM) quarks induces corrections to the SM quark couplings that are proportional to the square of the mixing angles [1, 2]. This has lead to the misconception that vector-like quarks cannot mix sizeably with first generation SM quarks, given the stringent constraints on SM quark couplings from precision flavor and electroweak (EW) observables. Motivated by models with warped extra dimensions [3, 4] it was pointed out in Ref. [5] that when first generation SM quarks mix with several new quarks with different quantum numbers, the contributions of the different multiplets to the anomalous SM quark couplings can cancel among themselves, thus leaving no low energy trace even for large values of mixing. These cancellations can in fact be enforced by a symmetry [6] naturally present in composite Higgs models with minimal flavor violation [7]. Indirect constraints provide only mild restrictions in these models and the direct searches advocated in Refs. [5, 8] and recently performed in Refs. [9, 10] become the main probes of these new vector-like quarks.

The prototypical example in which these cancellations are present is the degenerate bidoublet model. It contains four new quarks, two with electric charge $2/3$, one with electric charge $5/3$ and the last one with electric charge $-1/3$. These new quarks have a unique decay mode to the up quark and the Z , H , W^+ and W^- bosons, respectively, all with 100% branching fraction. Current direct searches involve only decay modes involving EW gauge bosons and are therefore sensitive to three out of the four quarks in the model. In this article we study for the first time the ability of the Large Hadron Collider (LHC) to measure the Higgs channels in the degenerate bidoublet model. These channels are crucial to fully test the nature of the model. Higgs channels relying on the presence of new particles beyond the heavy quarks (a massive color octet vector boson) have been recently studied in the degenerate bidoublet model in the context of composite Higgs models in Ref. [11]. In this article we consider the minimal case in which the four new quarks are the only new particles at the relevant energies.

New quarks can be pair or singly produced. Pair production is dominated by QCD interactions and is therefore model-independent. It is however not directly sensitive to the coupling between the new quarks and the SM quarks but only to the corresponding branching fractions. Furthermore, for sizeable values of the mixing angles that we are interested in single production is actually a more sensitive probe of these models as shown in Refs. [5, 8] and also by current experimental limits in each channel [10, 12]. Thus, we disregard pair production in this article and focus on single production. Single production can proceed via different mechanisms. The most relevant ones in the model under consideration are t -channel exchange of the Higgs boson, single production through fusion of the Higgs and an EW gauge boson and single production in association with a Higgs boson. We will show that the latter two production mechanisms have a good reach at the LHC and are capable of providing an important test of the model if it is realized in nature. Given current constraints from single production in the EW gauge boson channels we focus on the LHC running at its highest designed luminosity with $\sqrt{s} = 14$ TeV.

The rest of the article is organized as follows. We describe the model and its main features in Section II. We then discuss the main processes involving the Higgs channels in the model in Section III and dedicate Sections IV and V to the detailed analysis of the LHC reach in the two most promising channels: vector-boson fusion and associated production. Finally

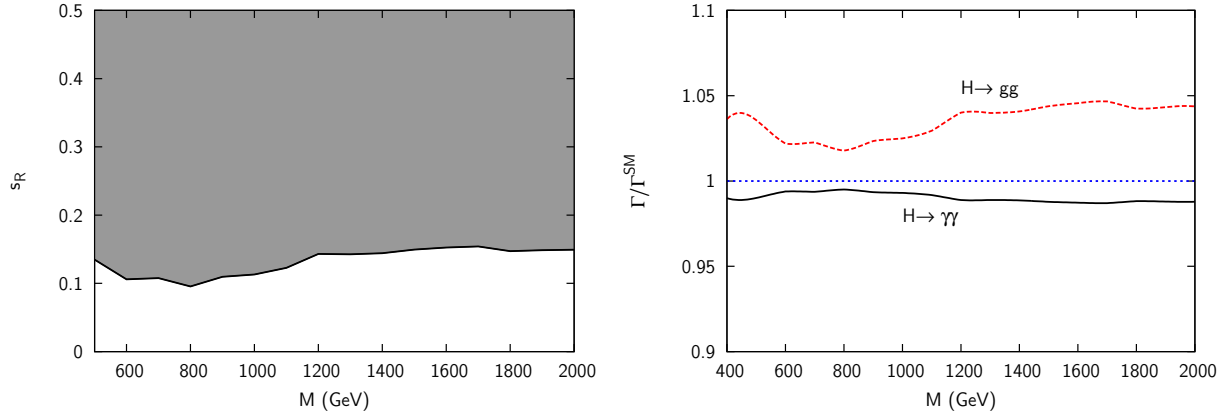


FIG. 1: (a) Left: upper bound on the value of the mixing angle, s_R , as a function of the common heavy quark mass, M , for the degenerate bidoublet derived from direct searches [10]; (b) right: Maximum deviation of Higgs decay widths $\Gamma(H \rightarrow gg, \gamma\gamma)$ with respect to the SM in the degenerate bidoublet model when the bounds from direct searches (left panel) are taken into account.

we discuss our results and conclude in Section VI.

II. DEGENERATE BIDOUBLET MODEL: DEFINITION AND CONSTRAINTS

The degenerate bidoublet model has been described in full detail in Refs. [5, 8] (for an implementation in the lepton sector see Ref. [13, 14]). It consists of two new vector-like doublet quarks of hypercharges $1/6$ and $7/6$, respectively, with identical Dirac mass, that mix with equal strength only with the up quark in the basis in which all the non-trivial flavor structure resides in the down sector. The spectrum includes two charge $2/3$ quarks (denoted by U_Z , U_H), one of charge $5/3$ (denoted by X) and one of charge $-1/3$ (denoted by D). All observables can be parameterized in terms of two masses, that we take to be m_u , the SM up quark mass and the common mass $M = m_{U_Z} = m_D = m_X$, and a mixing angle $s_R \equiv \sin \theta_R$. The relevant relations between these parameters are

$$\begin{aligned} m_{U_H} &= M c_L / c_R, \quad s_L = s_R m_u^2 / M^2 \approx 0, \\ \kappa_{uU_Z}^R &= \sqrt{2} \kappa_{uX}^R = \sqrt{2} \kappa_{uD}^R = s_R, \quad y_{uU_H}^R = s_R c_R \frac{m_{U_H}}{v}. \end{aligned} \quad (1)$$

All other couplings are either vanishing or suppressed by powers of s_L and therefore negligible. From these couplings it should be clear from the choice of notation, the only allowed decays for the charge $2/3$ quarks are $U_Z \rightarrow Zu$ and $U_H \rightarrow Hu$. Similarly, X and D can only have charged current decays. This model enjoys a custodial symmetry protection of the SM quark gauge couplings. They only receive corrections proportional to powers of $|s_L| \lesssim 10^{-11}$ from the mixing with the new quarks. One loop constraints give the very mild bound [8]

$$|s_R| \lesssim 0.75. \quad (2)$$

Direct searches result in the most stringent constraints for the degenerate bidoublet model. We have translated the constraints obtained in Ref. [10] to the degenerate bidoublet case and the results are shown in Fig. 1(a). In Ref. [10] the bounds were obtained assuming

only one type of quark at a time. In our model we have only one quark, U_Z , contributing to the neutral current channel, and therefore the experimental bound as given in Ref. [10] applies to our analysis as well. However for the charged current channel we have two quarks, X and D , contributing simultaneously whereas in Ref. [10] only one quark was considered. Hence in extracting the limits on the coupling we have to consider the case that both quarks are simultaneously present. The explicit expressions for including different types of quarks are given in Ref. [8]. The bound presented in Fig. 1(a) is the most stringent one of the charged and neutral current channels. These constraints are stringent enough that Higgs searches do not impose any further constraints. For instance, given the current bounds in Fig. 1(a), gluon fusion is enhanced with respect to the SM by less than 5% and the $h \rightarrow \gamma\gamma$ channel decreased by less than 2% as shown in Fig. 1(b). These direct constraints on s_R also imply that $m_{U_H} \approx M$ with an approximate precision of 1%, well within the experimental resolution. Thus, from now on we will consider all four quarks to be degenerate.

III. HIGGS PRODUCTION CHANNELS

We describe in this section the relevant single production mechanisms of new quarks that involve at least one Higgs boson in the final state in the context of the degenerate bidoublet model. One important feature of the model is the fact that each of the heavy quarks couples to the u quark and only one gauge boson or the Higgs, *i.e.* $Br(X \rightarrow uW^+) = Br(U_Z \rightarrow uZ) = Br(D \rightarrow uW^-) = Br(U_H \rightarrow uH) = 100\%$. This strongly restricts the number of relevant diagrams that contribute to Higgs production through the decay of the heavy quark U_H . The three mechanisms that we consider and their relevant features are:

- *Single production:* $qq' \rightarrow jU_H \rightarrow jjH$.
In this channel the heavy quark, U_H , is produced in association with a single (forward) jet. Subsequent decay of the heavy quark to a jet and the Higgs boson leads to a final state of Hjj as shown in Fig. 2(a). Single production is suppressed in our model by the up quark Yukawa coupling and will be disregarded henceforth.
- *Vector boson Higgs fusion (VBHF):* $qq' \rightarrow jVU_H \rightarrow jjVH$, where $V = W, Z$.
In this channel the heavy quark, U_H , is produced in association with a (forward) jet and an EW gauge boson. After the decay of the heavy quark we have a final state of $VH+2j$, where $V = W, Z$ gauge boson as shown in Fig. 2(b). The VBHF production mechanism is initiated by two valence quarks, involves unsuppressed couplings and has a longitudinal gauge boson enhancement. Thus, the corresponding cross section can be sizeable and relatively insensitive to the mass of the heavy quark. This is shown in Fig. 3 where the cross sections correspond to the currently allowed values of s_R . The presence of an EW gauge boson allows for a clean trigger using its leptonic decays thereby allowing the use of the dominant $b\bar{b}$ Higgs decay.
- *Associated Production:* $qg \rightarrow HU_H \rightarrow jHH$.
In this channel the heavy quark, U_H is produced in association with a Higgs boson and the subsequent decay of the heavy quark leads to a unique two Higgs plus a hard jet final state shown in Fig. 2(c). Double Higgs production has been studied as a way of measuring Higgs self-couplings [15–17] and anomalous Higgs couplings [18–20]. The presence of a hard jet from the decay of the heavy quark in our analysis enhances signal over background. Associated production is initiated by a valence quark and a

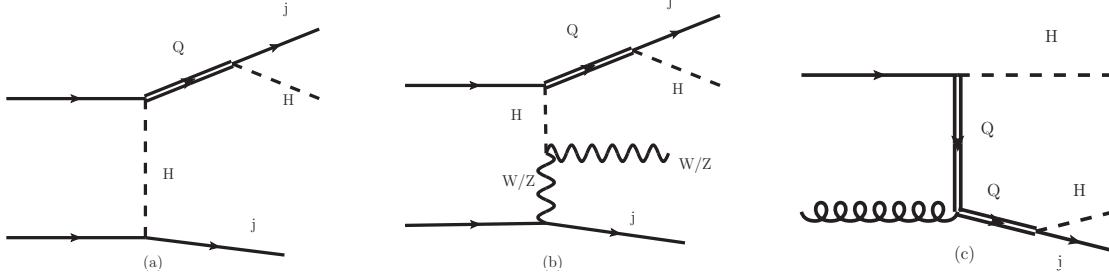


FIG. 2: Sample diagrams for: (a) single production, (b) vector boson Higgs fusion and (c) associated production of U_H with subsequent decay into Hu .

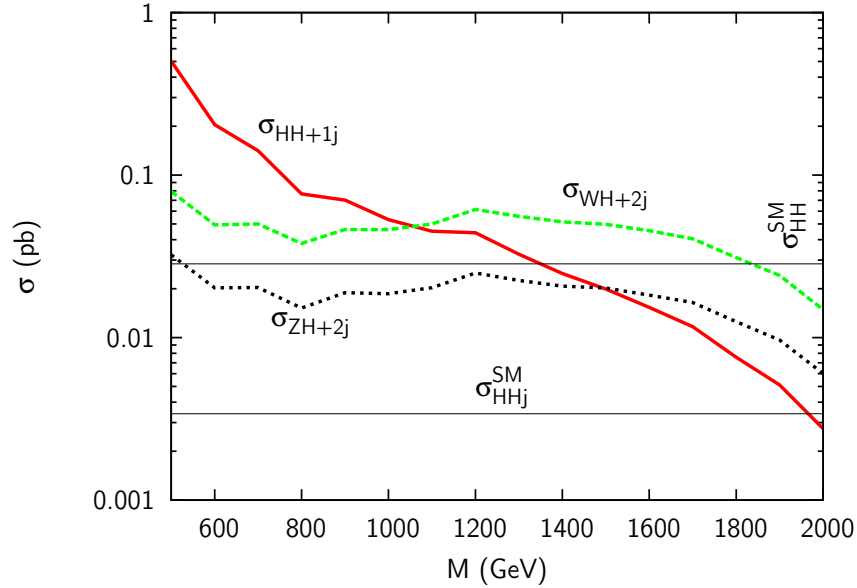


FIG. 3: Cross sections (in pb) for the associated production channel (labeled $HH+1j$) and the vector boson Higgs fusion channel (labeled $WH+2j$ or $ZH+2j$) for s_R fixed to the current upper bound. For reference we also show the SM production cross section of two Higgs bosons and two Higgs bosons plus a hard jet with $p_T(j) > 100$ GeV.

gluon. Hence the cross sections can be quite large for small values of M but suffer a stronger suppression for larger values of the heavy quark mass, due to the steeply falling gluon parton distribution functions (PDFs). We show the cross section for this process in Fig. 3 for the currently allowed values of s_R . For comparison we also show in Fig. 3 the production cross section for $HH + X$ and $HH + j + X$ in the SM, with $p_T(j) \geq 100$ GeV, as computed in [16].

In the following two sections we describe the analyses we propose to measure the VBHF and associated production mechanisms. We have generated signal and background events at partonic level using **Madgraph** v 4.5.0 [21] and **ALPGEN** v2.13 [22], respectively. We have then used **Pythia** v 6.4 [23] for hadronization and showering and **Delphes** v 1.9 [24] for fast detector simulation. The detector card in **Delphes** has been modified to better agree with published distributions [25–27]. The main changes are: the tracking efficiency was

Background	$\sigma(pb)$	Background	$\sigma(pb)$
$t\bar{t}$ semileptonic + 0 - 4j	222.3	$W_{\ell\nu}WW + 0 - 2j$	0.14
$t\bar{t}$ fully leptonic + 0 - 4j	54.3	$WWZ + 0 - 2j$	0.18
$W_{\ell\nu}b\bar{b} + 0 - 2j$	12.5	$W_{\ell\nu} + 1j, p_T^{j_h} > X$	178.1
$b\bar{b}b\bar{b} + 1j, p_T^{j_h} > X$	3.1	$t\bar{t}b\bar{b}$	0.85
$b\bar{b} + 3j$	515.0	$W_{\ell\nu}W + 0 - 2j$	49.0
$Z_{\ell\ell}/\gamma_{\ell\ell} + 1 - 4j$	552.7	$WZ + 0 - 2j$	39.9
$Z_{\ell\ell}Z + 0 - 2j$	2.37	$Z_{\ell\ell}b\bar{b} + 0 - 2j$	4.5

TABLE I: Cross sections (in pb) for the various background processes. In our notation $W_{\ell\nu}$ and $Z_{\ell\ell}$ represent leptonic decays of the W and Z gauge bosons and $\ell = e, \mu, \tau$. The transverse momentum cut for the hardest jet (j_h) for W +jets background is $X = 130$ GeV. In the case of $b\bar{b}b\bar{b} + 1j$ we have $X = 150$ GeV. The explicit number of jets listed stands for the ones generated at the parton level and the rest of the jets are from initial and final state radiation. The first three are the main backgrounds to the VBHF channel and the next two are the main ones for the $4b+j$ associated production channel. The other background processes listed in the table have been considered in the analysis but become irrelevant after all the optimization cuts have been applied.

updated to 95; the isolation criterion was changed to $\Delta R = 0.4$ and a value of 0.7 was used for the b -tagging efficiency. We have used the CTEQ6L1 PDFs [28] and use M for factorization and renormalization scales for signal and the default values for background. Thus, $\sum m_Q^2 + p_T^2$ was used for $Q\bar{Q}$ +jets and $Q\bar{Q}Q\bar{Q}$ +jets (with $Q = b, t$), where the sum extends to all the final state partons, while $m_V^2 + p_{T,V}^2$ was used for V +jets (with $V = W, Z$). Jets and leptons are defined as requiring $p_T^j > 30$ GeV, $|\eta_j| < 5$, $p_T^\ell > 20$ GeV, $|\eta_\ell| < 2.5$ and $\Delta R(j\ell) > 0.4$, where jets are clustered using the anti- k_T algorithm using a cone radius of $\Delta R = 0.4$. Throughout the analysis we have used the Higgs mass to be $m_H = 125$ GeV. We show in Table I the relevant backgrounds for the analyses in this article with their corresponding cross sections.

IV. VECTOR BOSON HIGGS FUSION

In the vector boson Higgs fusion channel the heavy quark, U_H , is produced singly in association with a W or Z gauge boson and a jet leading to the final state

$$pp \rightarrow VU_H j \rightarrow V H j j, \quad (3)$$

where $V = W, Z$. Of the two jets in the final state, the one coming from the heavy quark decay tends to be quite hard whereas the other one tends to be relatively forward. Furthermore the Higgs boson comes from the decay of a massive particle (U_H) and is typically quite boosted. These features can be used to enhance signal over backgrounds. Considering the leptonic decays of the gauge boson helps reduce QCD backgrounds as well as provide a clean trigger. Hence we will consider only the leading $H \rightarrow b\bar{b}$ decay. The final state is therefore $b\bar{b}jj\ell\ell$ or $b\bar{b}jj\ell\ell$, for $V = W$ or Z gauge boson respectively. The latter process is potentially cleaner but suffers from reduced statistics. The cross section is of $\mathcal{O}(fb)$ once the decay branching fractions of the Z and H are included. Thus, even a minimal set of

M (GeV)	σ_s (fb)	ϵ_s	$\epsilon_{t\bar{t}}$	$\epsilon_{Wb\bar{b}}$
500	79	0.010	1.0×10^{-4}	1.4×10^{-4}
1000	46	0.040	4.7×10^{-5}	7.7×10^{-5}
1500	50	0.025	7.7×10^{-6}	1.4×10^{-5}

TABLE II: Cross sections (in fb) for the signal ($WHjj$) and efficiencies for signal and main backgrounds for different values of M . The corresponding background cross sections are listed in Table I.

cuts quickly reduces the number of events to just a few except for very large luminosities. For this reason we focus on the more promising charged current channel.

A. Charged current channel

For the charged current channel with the $b\bar{b}jj\ell\cancel{E}_T$ final state we have implemented the following cuts:

- Particles: exactly one charged lepton (e or μ) plus at least four jets with exactly two b tags.
- Hard jet: $p_T(j_h) \geq 200$ GeV for the hardest jet that is not b-tagged.
- Higgs reconstruction: $|m_{bb} - m_H| \leq 30$ GeV.
- Higgs boost: $\Delta R(bb) \leq 1$.
- Heavy quark mass: $|m_{bbj_h} - M| \leq 200$ GeV.

We show in Table II the signal cross section and the total efficiencies for the signal and main backgrounds for different values of the heavy quark mass. All relevant background processes have been considered but we only report the ones that are non-negligible after all the cuts in Table II. In Fig. 4(a) we show the 2 and 5σ sensitivity for the production cross section times branching fraction for the $WHjj$ channel as a function of the heavy quark mass, M , for the LHC with $\sqrt{s} = 14$ TeV and an integrated luminosity of 300 fb^{-1} . For reference we also show the current (95% C.L.) upper bound (indicated by the dotted blue curve) in the context of the degenerate bidoublet model. In Fig. 4(b) we show the confidence level that can be reached, as a function of M for different values of total integrated luminosity when s_R is fixed to the current upper limit. As seen in Fig. 4 new regions in parameter space that are currently unconstrained can be probed in the early runs with 10 (50) fb^{-1} at 2 (5) σ sensitivity. The shape of the contours in these figures can be understood from the production cross section, which is flat as a function of M as shown in Fig. 3. Larger values of M give rise to a similar number of signal events but the requirement on the heavy quark mass reconstruction reduces the background more efficiently for higher masses of the heavy quark. For $M \gtrsim 1.5$ TeV the production cross section decreases due to the decreased parton luminosity and so does the sensitivity.

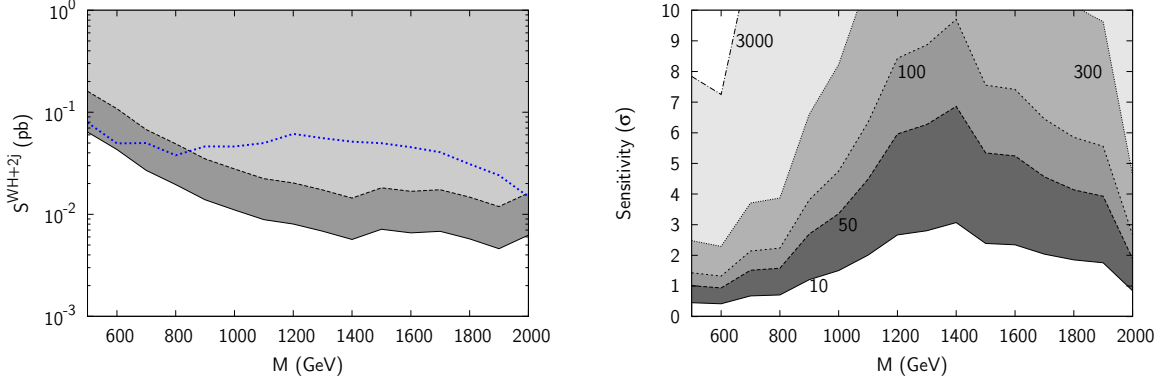


FIG. 4: (a) Left: 2 and 5σ bounds (indicated by dark and light colored regions respectively) on the production cross section times branching fraction for the $WHjj$ channel as a function of the heavy quark mass, M , for the LHC with $\sqrt{s} = 14$ TeV and an integrated luminosity of 300 fb^{-1} . For reference we also show the current (95% C.L.) upper bound (indicated by the dotted blue curve) in the context of the degenerate bidoublet model. (b) right: contour plot of the luminosity required for a certain degree of confidence level as a function of the heavy quark mass in the degenerate bidoublet model with s_R fixed to the current limit.

V. ASSOCIATED PRODUCTION

In the associated production channel, the heavy quark, U_H , is produced in association with a Higgs boson as shown in Fig. 2(c). Subsequent decay of the heavy quark leads to the unique final state with two Higgs bosons and a hard jet:

$$pp \rightarrow HU_H \rightarrow HHj. \quad (4)$$

Double Higgs production has received some attention as a means of measuring the Higgs self-couplings in the SM, see for instance Refs. [15–17]. In the case of the SM, this is a very difficult measurement at the LHC due to the very low cross section, $\sigma_{SM}(pp \rightarrow HH + X) = 28.4 \text{ fb}$ [16]. As shown in Fig. 3 the double Higgs production cross section can be larger (by up to an order of magnitude for the lowest masses) in our model for masses $M \lesssim 1.4$ TeV. Furthermore, the presence of a very hard jet from the decay of the heavy quark in our model provides better signal sensitivity over background. In fact, even for the lowest value of the masses considered, in over 90 % of the signal events the hardest jet has $p_T(j_h) \geq 100$ GeV whereas in the SM the corresponding cross section goes down to $\sigma_{SM}(p \rightarrow HHj + X; p_T^j \geq 100 \text{ GeV}) = 3.2 \text{ fb}$. Even without the extra hard jet it has been argued recently that the LHC can be sensitive to double Higgs production in models beyond the SM with anomalous Higgs couplings [18–20] with an enhancement factor with respect to the SM cross section similar to the one present in our model. Hence our analysis which probes the underlying structure of the degenerate bidoublet model is competitive with the other double Higgs studies (which probe different theoretical aspects).

The presence of two Higgs bosons can lead to different final states based on the decay modes of the Higgs. We will consider two scenarios: one where both Higgs bosons decay to $b\bar{b}$ and the other where one Higgs boson decays to $b\bar{b}$ and the other to a pair of photons. This gives rise to the final states $b\bar{b}b\bar{b}j$ and $b\bar{b}\gamma\gamma j$ respectively. In the following sections we will estimate the LHC reach for the associated production channel with the two final states

mentioned above in the context of the degenerate bidoublet model.

A. $b\bar{b}\gamma\gamma$ channel

The $b\bar{b}\gamma\gamma$ channel has been studied in detail in Ref. [15] in the context of the SM and in Ref. [19] in models with anomalous di-Higgs couplings like composite Higgs models. The result is that the cross section is too small for a reasonable measurement in the SM but in some composite Higgs models one could reach discovery in this channel for values of the cross section $\sigma(pp \rightarrow HH \rightarrow b\bar{b}\gamma\gamma) \gtrsim 6 \times \sigma(pp \rightarrow HH \rightarrow b\bar{b}\gamma\gamma)^{SM}$ [19]. In our model there are regions of parameter space in which the double Higgs production cross section is enhanced by an even larger factor with respect to the SM, even before taking into account the presence of a hard jet. In order to estimate the LHC reach we have generated events for the signal and the irreducible background. We have implemented the following cuts as suggested in Ref. [15]:

- Two b-tagged jets and two photons satisfying

$$\begin{aligned} p_T(b) &> 45 \text{ GeV}, \quad |\eta(b)| < 2.5, \quad \Delta R(b, b) > 0.4, \\ p_T(\gamma) &> 20 \text{ GeV}, \quad |\eta(\gamma)| < 2.5, \quad \Delta R(\gamma, \gamma) > 0.4, \\ |m_{bb} - m_H| &< 20 \text{ GeV}, \quad |m_{\gamma\gamma} - m_H| < 2.3 \text{ GeV}, \quad \Delta R(\gamma, b) > 0.4. \end{aligned} \quad (5)$$

- Angular cuts

$$\Delta R(b, \gamma) > 1.0, \quad \Delta R(\gamma, \gamma) < 2.0. \quad (6)$$

Finally we also impose an extra cut on the p_T of the hardest jet to further reduce the background:

$$p_T(j_h) > 100 \text{ GeV}. \quad (7)$$

The signal and irreducible background efficiencies for the cuts in Eq. (5) - (7) are shown in Table III. Note that the cut on the p_T of the hard jet is rather conservative since a larger cut such as $p_T(j_h) > 300 \text{ GeV}$ would reduce the background significantly while preserving most of the signal. The cross section for the irreducible background after the cuts of Eq. (5) and Eq. (6) agree with those in Refs. [15, 19] to within $\mathcal{O}(15\%)$. Given this agreement we use the efficiencies for the reducible (subleading) backgrounds from Refs. [15, 19] and assume the same efficiency for the cut on the p_T of the hard jet as in the irreducible background. We use the resulting efficiencies to estimate the 2 and 5σ reach for this channel at the LHC with $\sqrt{s} = 14 \text{ TeV}$ for 300 fb^{-1} of integrated luminosity and the results are shown in Fig. 5(a). For comparison the current bound in the degenerate bidoublet model as obtained from single EW production is also shown as the blue dotted curve. In Fig. 5(b) we show the confidence level as a function of the heavy quark mass for different values of total integrated luminosity when s_R is fixed to the current upper bound. We see that with an integrated luminosity of 300 fb^{-1} we can obtain a 2 (5) σ measurement up to 1.4 (1.0) TeV.

B. $b\bar{b}b\bar{b}$ channel

Next we turn our attention to the channel with the largest branching fraction, the one in which both Higgs bosons decay into $b\bar{b}$. *A priori* a channel with only jets in the final state

cut	ϵ_{800}	ϵ_{1600}	$\epsilon_{\text{irred.}}$
Eq.(5)	0.14	0.087	0.00023
Eq.(6)	0.76	0.7	0.13
Eq.(7)	0.99	1	0.011

TABLE III: Efficiencies for the signal (with $M = 800$ and 1600 GeV) and irreducible background in the $b\bar{b}\gamma\gamma$ channel for the various optimization cuts listed in Eqs. (5) - (7).

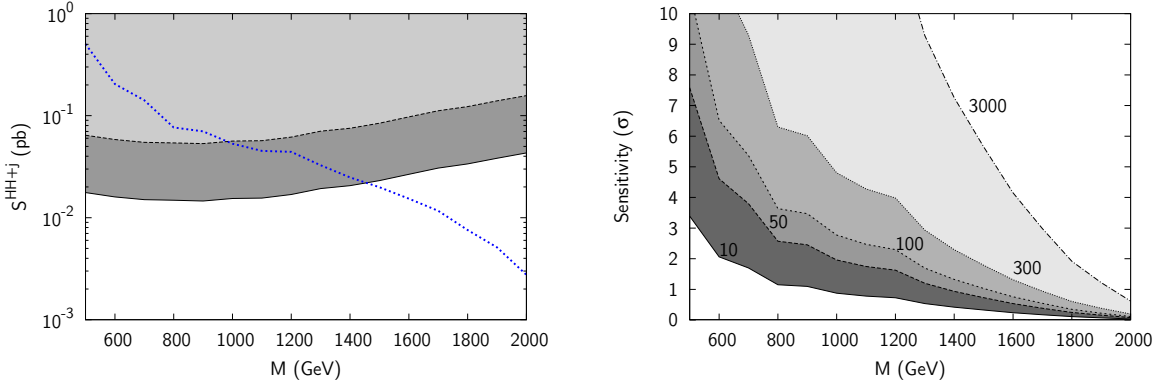


FIG. 5: Same as Fig. 4 but for the HHj channel with $b\bar{b}\gamma\gamma j$ final state.

is extremely challenging due to the immense QCD background. A realistic determination of the feasibility of this multijet channel would require computing resources and data-driven methods that are beyond the scope of this analysis. Hence we can only get a rough estimate of the LHC reach for this channel. In this study we aim to point out the unique features of this final state that will enhance signal sensitivity over the large backgrounds. These unique features include a very hard jet, four b quarks that reconstruct two Higgs bosons and the reconstructed heavy quark. We believe that our results are sufficiently promising to warrant a more detailed experimental study.

We have generated the following two background processes: the irreducible $b\bar{b}b\bar{b} + 1j$ and the $b\bar{b} + 3j$ backgrounds. The corresponding cross sections are shown in Table I. The huge background reduction resulting from the requirement of four b-tagged jets (we are assuming a fake tag rate of 1 %) allows us to neglect pure multijet QCD backgrounds.

We propose the following cuts:

- At least 5 jets, four of which must be tagged as b-jets.
- $p_T(j_h) > 300$ GeV.
- $|m_{jj} - m_H| < 50$ GeV (for both pairs of b-jets).

The very large $b\bar{b} + 3j$ cross section (see Table I) is greatly reduced due to the requirement of four b-tags, given the 1% mistag rate we consider. This huge reduction makes it very challenging to generate enough statistics to reasonably estimate the efficiency of the remaining cuts. In order to estimate this efficiency we have *not* imposed the requirement of the four b-tags but rescaled the corresponding cross sections with the factors resulting from the b-tagging efficiency ($\epsilon_{4b}(bbbbj) \approx 0.25$) or mistagging rate ($\epsilon_{4b}(bbjjj) \approx 1.5 \times 10^{-4}$). The remaining cuts on the transverse momentum of the hard jet and the Higgs mass reconstruction

are then implemented. The pairs of jets used to reconstruct the Higgs boson are selected from the four sub-leading jets, as in the signal the hardest jet is typically the one from the decay of U_H and is not a b quark. The two jets that reconstruct the Higgs mass closest to $m_H = 125$ GeV form the first pair while the remaining two jets reconstruct the other Higgs boson. Once the two Higgs candidates are selected we construct the invariant mass of one Higgs boson and the leading jet and require that at least one of these invariant masses be in the region

$$|m_{Hj_h} - M| < 400 \text{ GeV}. \quad (8)$$

We show the corresponding efficiencies after all cuts for the signal and the two backgrounds we have considered in Table IV and a summary of the results in Fig. 6. Keeping in mind the inherent lack of precision in the estimation of the backgrounds for this process we see that this channel is potentially even more promising than the $b\bar{b}\gamma\gamma$ one. A 2 (5) σ sensitivity could be obtained for masses up to 1.7 (1.3) TeV with 300 fb^{-1} integrated luminosity.

M (GeV)	σ_s (fb)	ϵ_s	ϵ_{4b+j}	ϵ_{2b+3j}	bk events/100 fb^{-1}
500	125	0.033	0.0051	0.0029	456
1000	12.6	0.057	0.005	0.003	412
1500	5.6	0.03	0.0008	0.0005	71

TABLE IV: Cross sections (in fb) for the signal ($b\bar{b}b\bar{b}j$ channel) and efficiencies for the signal and main backgrounds after all the cuts listed in the text for different values of heavy quark mass, M . The total number of background events with 100 fb^{-1} of integrated luminosity is also shown in the last column. The efficiency due to b-tagging as described in the text is not included in this table but it is used to compute the number of background events.

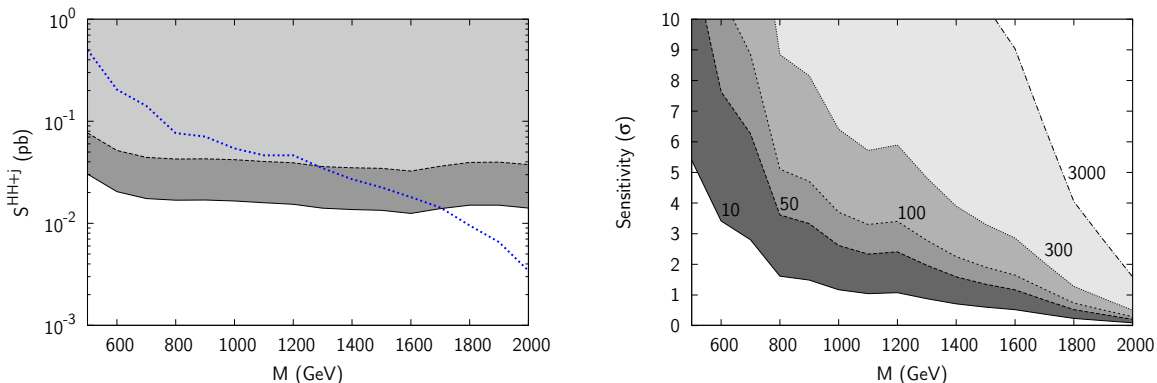


FIG. 6: Same as Fig. 4 but for the HHj channel with $b\bar{b}b\bar{b}j$ final state.

VI. DISCUSSION

New vector-like quarks can mix sizeably with first generation SM quarks without conflicting with current experimental constraints. The underlying mechanism that allows these new vector-like quarks to evade the very stringent indirect constraints requires more than one new quark so that delicate cancellations can take place. These cancellations can be

naturally enforced by symmetries that typically imply the new quarks to be degenerate and to have unique decays (with 100% branching fractions) into a SM quark and either an EW gauge boson or the Higgs boson. Channels involving new heavy quarks with decays into EW gauge bosons are currently being searched for at the LHC and have become the most stringent probes of these new quarks. The equivalence theorem however guarantees that if there are channels involving decays into EW gauge bosons then the channels with decays into the Higgs boson must also be present. Direct searches of the channels involving decays into the Higgs boson are therefore a crucial ingredient to fully disentangle the mechanism underlying the protection of the SM quark couplings in these new physics scenarios.

We have used as a benchmark a well motivated model that allows a large mixing of new vector-like quarks with first generation SM quarks, the so called degenerate bidoublet model. This model involves four new (essentially degenerate) quarks, each one decaying, with 100% branching fraction, into an up quark and a Z , H , W^+ and W^- , respectively. After discussing the current direct and indirect constraints on the model we have described the main production processes that involve the new quark with decays into a Higgs boson. We have proposed new searches that are sensitive to this type of new quark and have discussed the potential reach at the LHC.

The two most promising Higgs channels are vector boson Higgs fusion and associated production. The former channel results in a final state with a Higgs, an EW gauge boson and a hard jet. The charged current channel is particularly promising, with a reach of up to 2 TeV for the heavy quark mass with 300 fb^{-1} of integrated luminosity. In the associated production channel there are two Higgs bosons and a hard jet in the final state but it suffers from a smaller cross section. In the case where one Higgs boson decays into b quarks and the other into photons we have shown that a 5σ sensitivity can be reached with 300 fb^{-1} of integrated luminosity for a mass of the heavy quark below 1 TeV. We have also considered the case in which both Higgs bosons decay into $b\bar{b}$. Despite the all hadronic final state, the large number (four) of b quarks and a very hard extra jet are powerful enough discriminators to make this a very promising channel as well, with a reach of up to 1.3 TeV for the heavy quark mass with 300 fb^{-1} .

A measurement of new vector-like quarks that decay into the Higgs boson and a SM light quark would represent a crucial direct test of the underlying mechanism that protects the SM quark gauge couplings from large corrections. Our results show that this measurement is feasible at the LHC for a large portion of the currently allowed parameter space, in several different channels simultaneously.

Acknowledgments

This work has been partially supported by MICINN projects FPA2006-05294 and FPA2010-17915, through the FPU program and by Junta de Andalucía projects FQM 101, FQM 03048 and FQM 6552. AA is supported by the United States National Science Foundation under grant PHY-0854889.

-
- [1] F. del Aguila and M. J. Bowick, Nucl.Phys. **B224**, 107 (1983).
 - [2] F. del Aguila, M. Perez-Victoria, and J. Santiago, JHEP **0009**, 011 (2000), hep-ph/0007316.

- [3] M. S. Carena, E. Ponton, J. Santiago, and C. E. Wagner, Nucl.Phys. **B759**, 202 (2006), hep-ph/0607106.
- [4] M. S. Carena, E. Ponton, J. Santiago, and C. Wagner, Phys.Rev. **D76**, 035006 (2007), hep-ph/0701055.
- [5] A. Atre, M. Carena, T. Han, and J. Santiago, Phys.Rev. **D79**, 054018 (2009), 0806.3966.
- [6] K. Agashe, R. Contino, L. Da Rold, and A. Pomarol, Phys.Lett. **B641**, 62 (2006), hep-ph/0605341.
- [7] M. Redi and A. Weiler, JHEP **1111**, 108 (2011), 1106.6357.
- [8] A. Atre, G. Azuelos, M. Carena, T. Han, E. Ozcan, et al., JHEP **1108**, 080 (2011), 1102.1987.
- [9] G. Aad et al. (ATLAS Collaboration), Phys.Lett. **B712**, 22 (2012), 1112.5755.
- [10] Tech. Rep. ATLAS-CONF-2012-137, ATLAS-COM-CONF-2012-167, CERN, Geneva (2012).
- [11] A. Carmona, M. Chala, and J. Santiago, JHEP **1207**, 049 (2012), 1205.2378.
- [12] G. Aad et al. (ATLAS Collaboration), Phys.Rev. **D86**, 012007 (2012), 1202.3389.
- [13] F. del Aguila, A. Carmona, and J. Santiago, Phys.Lett. **B695**, 449 (2011), 1007.4206.
- [14] A. Carmona and F. Goertz (2013), 1301.5856.
- [15] U. Baur, T. Plehn, and D. L. Rainwater, Phys.Rev. **D69**, 053004 (2004), hep-ph/0310056.
- [16] M. J. Dolan, C. Englert, and M. Spannowsky, JHEP **1210**, 112 (2012), 1206.5001.
- [17] F. Goertz, A. Papaefstathiou, L. L. Yang, and J. Zurita, JHEP **1306**, 016 (2013), 1301.3492.
- [18] R. Grober and M. Muhlleitner, JHEP **1106**, 020 (2011), 1012.1562.
- [19] R. Contino, M. Ghezzi, M. Moretti, G. Panico, F. Piccinini, et al., JHEP **1208**, 154 (2012), 1205.5444.
- [20] M. J. Dolan, C. Englert, and M. Spannowsky (2012), 1210.8166.
- [21] J. Alwall et al., JHEP **09**, 028 (2007), 0706.2334.
- [22] M. L. Mangano, M. Moretti, F. Piccinini, R. Pittau, and A. D. Polosa, JHEP **0307**, 001 (2003), hep-ph/0206293.
- [23] T. Sjostrand, S. Mrenna, and P. Z. Skands, JHEP **0605**, 026 (2006), hep-ph/0603175.
- [24] S. Oryn, X. Roubey, and V. Lemaitre (2009), 0903.2225.
- [25] F. Hubaut, E. Monnier, P. Pralavorio, K. Smolek, and V. Simak, Eur.Phys.J. **C44S2**, 13 (2005), hep-ex/0508061.
- [26] F. Hubaut, E. Monnier, P. Pralavorio, B. Resende, and C. Zhu (2006).
- [27] N. Castro, Ph.D. thesis, Univ. Coimbra, Coimbra (2008), presented on 17 Oct 2008, CERN-THESIS-2008-083.
- [28] J. Pumplin, D. Stump, J. Huston, H. Lai, P. M. Nadolsky, et al., JHEP **0207**, 012 (2002), hep-ph/0201195.